

000 ICECACHE: MEMORY-EFFICIENT KV-CACHE MANAGE- 001 002 MENT FOR LONG-SEQUENCE LLMS 003 004

005 **Anonymous authors**

006 Paper under double-blind review

007 008 ABSTRACT 009

011 Key-Value (KV) cache plays a pivotal role in accelerating inference in large lan-
012 guage models (LLMs) by storing intermediate attention outputs, thereby avoiding
013 redundant computation during auto-regressive generation. However, the cache’s
014 memory footprint scales linearly with sequence length, often resulting in memory
015 bottlenecks on constrained hardware. While prior work has explored offloading KV-
016 cache to the CPU and maintaining a reduced subset on the GPU, these approaches
017 frequently suffer from imprecise token prioritization and degraded performance in
018 long-generation tasks such as multi-turn dialogues and chain-of-thought reasoning.
019 In this paper, we propose a novel KV-cache management strategy called IceCache,
020 that integrates semantic token clustering with PagedAttention, a memory-efficient
021 paging mechanism. By clustering semantically related tokens and organizing them
022 into a hierarchical, dynamically updateable structure, our method improves cache
023 hit rates and memory bandwidth utilization during CPU-GPU transfers. Experi-
024 mental results show that IceCache achieves over 99% accuracy with a 256-token
025 budget and still maintains 97% accuracy with only a 64-token budget, compared
026 to the full KV-cache model. It outperforms existing baselines even while using
027 just 25% of the KV-cache token budget, demonstrating its superior accuracy in
028 long-sequence scenarios.

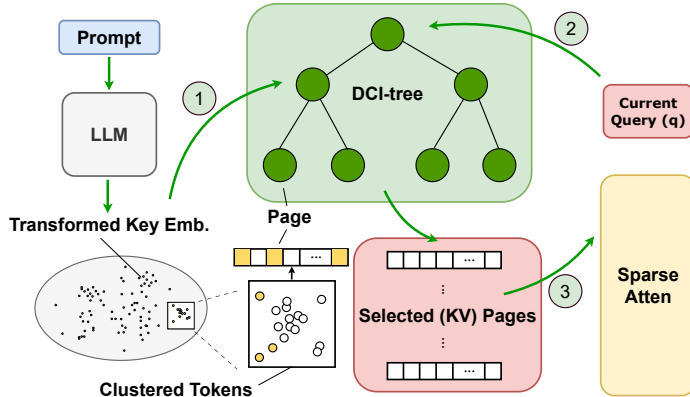
029 1 INTRODUCTION 030

031 Key-Value (KV) cache is a critical component in modern large language models (LLMs) which stores
032 the intermediate attention outputs for each token, allowing the model to reuse these computations
033 in subsequent forward passes. This is particularly important for auto-regressive generation tasks,
034 where tokens are generated one at a time. By caching these values, the model avoids redundant
035 calculations, dramatically reducing the runtime required for generating long sequences. However, the
036 main challenge for a KV cache lies in its memory consumption. As the generated sequence grows
037 longer, the required cache size increases linearly, potentially leading to out-of-memory errors on
038 devices with limited RAM.

039 Recent research (Zhang et al., 2024b; Tang et al., 2024; Xiao et al., 2023) has revealed that despite
040 the growing size of the KV cache, a small subset of tokens plays a disproportionately important
041 role in maintaining generation accuracy. This insight suggests that we can significantly reduce
042 inference time by selectively loading only these crucial tokens, without compromising the quality of
043 the output. Some research (Chen et al., 2024a; Lee et al., 2024; Chen et al., 2024b) takes this approach
044 further by offloading the KV-cache to the CPU and dynamically maintaining a subset of the most
045 significant KV-cache on the GPU. However, many previous methods do not identify and prioritize
046 these critical parts of the KV-cache in a precise way so that the hit rate of the truly important tokens
047 is low. Therefore, in scenarios involving long-generation tasks, such as long-context summarization,
048 multi-step reasoning, and extended chain-of-thought (CoT) generation, previous methods experience
049 significant performance degradation (Li et al., 2024a).

050 To improve the identification of critical parts of the KV-cache, we propose an innovative approach,
051 which we call IceCache, that integrates token clustering with a currently prevalent method – Page-
052 dAttention (Kwon et al., 2023) which stores the KV-cache in non-contiguous paged memory. As
053 illustrated in Figure 1, by grouping semantically related tokens into pages, our approach aims to
enhance the hit rate when selecting critical pages and tokens, and increase the transmission bandwidth

054 during the GPU-CPU offloading for the pages. Additionally, by employing a hierarchical data
 055 structure that can be efficiently updated during the decoding phase, we can mitigate the performance
 056 degradation commonly observed in long-generation tasks in previous studies. This leads to more
 057 effective use of the KV-cache, especially in the long-generation setting. IceCache is beneficial in two
 058 scenarios: (1) it achieves better accuracy than state-of-the-art methods using the same budget size;
 059 (2) it achieves comparable accuracy using a much smaller budget size (as small as 25%).
 060



074 Figure 1: **Illustration of IceCache.** (1) During the prefill stage, tokens are indexed into a tree structure
 075 (**the DCI-tree**) according to their semantic similarity in the transformed key-embedding space. Each
 076 leaf node of the DCI-tree corresponds to a physical memory page. (2) During the decoding stage,
 077 given a query q , IceCache performs a tree search to identify the top- k tokens most relevant to q . The
 078 zoomed-in section at the bottom illustrates that these critical tokens (highlighted in yellow) tend to be
 079 clustered within the same leaf nodes and are stored together in corresponding memory pages. (3)
 080 After the query-aware token search, the pages (leaf nodes) containing the critical tokens are selected,
 081 and all tokens within these pages are utilized in the subsequent sparse attention with q .
 082

083 IceCache has the following contributions:

084 **1. Token Clustering for Efficient Storage:** In the Prefill stage, instead of storing the KVs sequentially
 085 in their original order, we first cluster the tokens based on their similarity in a transformed key-
 086 embedding space using a maintainable tree-structured index, called DCI-tree. Tokens belonging to
 087 the same cluster are then stored together in the same memory page(s).

088 **2. Query-aware Critical Page Selection:** In the Decoding stage, given a specific query, only a subset
 089 of pages for each head are loaded to GPU to perform the attention computation for each layer and
 090 attention head. These pages are selected based on the presence of critical tokens, which is decided by
 091 an Approximated Nearest Neighbour (ANN) algorithm called Multi-level DCI (M-DCI).

092 **3. Efficient Pipelining with CPU-GPU overlapping:** IceCache performs M-DCI-based indexing
 093 and page selection on the CPU in parallel with GPU operations such as attention computation and
 094 feedforward layer execution. This pipelined design effectively overlaps computations, hiding much
 095 of the latency introduced by page selection.

097 We evaluated IceCache under constrained GPU memory budgets on the Passkey Retrieval (Mo-
 098 htashami & Jaggi, 2023), LongBench (Bai et al., 2023), and GSM8K Chain-of-Thought (CoT)
 099 reasoning (Wei et al., 2022) using four popular open-source LLMs: Llama3.1-8B-Instruct, Mistral-
 100 7B-Instruct-v0.2, LongChat-7B-v1.5 and Qwen3-32B. Across diverse tasks, including open-domain
 101 QA, multi-hop reasoning, academic reading comprehension, long-context summarization and long-
 102 context generation, IceCache consistently outperformed six state-of-the-art KV-cache baselines.
 103 Notably, IceCache sustained near-oracle performance (over 99%) on most tasks using only a small
 104 fraction (as small as 64 tokens) of the original KV cache size. For instance, on the challenging
 105 *GovReport* task, known for its long-range dependencies and high generation demands, IceCache
 106 achieved accuracy within 1% of the full KV baseline, whereas other methods experienced sharp
 107 performance drops. Furthermore, by leveraging its hierarchical index and well-designed pipelining,
 108 IceCache achieves decoding speedups comparable to leading baselines, demonstrating both efficiency
 109 and scalability for long-context LLM inference.

108

2 RELATED WORK

109

110 Lots of recent methods have aimed to enhance the efficiency of attention mechanisms in large language
111 models, especially for handling long-context inputs. H2O (Zhang et al., 2024b) only keeps a subset
112 of tokens selected by the attention scores to save memory for the KV-cache. StreamingLLM (Xiao
113 et al., 2023) utilizes the initial tokens, which they call sink tokens and the most recent tokens to
114 accelerate the attention computation. Methods such as SparQ (Ribar et al., 2023) apply approximate
115 attention by only selecting important indices across the head dimension. Similarly, MagicPiG (Chen
116 et al., 2024b) employs a sampling technique to provide a faithful estimation of the attention output.
117 OmniKV (Hao et al., 2025) reduces memory overhead by reusing the important tokens identified
118 across consecutive layers. SnapKV (Li et al., 2024b) uses the last portion of the prompt to select
119 the important key embeddings for the following decoding. PQCache (Zhang et al., 2024a) employs
120 product quantization to manage KV-cache and approximate the attention computation.
121

122 PagedAttention (Kwon et al., 2023) is an innovative memory management technique designed to
123 optimize the KV-cache of LLMs. It addresses the challenges by introducing a paging mechanism
124 similar to virtual memory systems in operating systems. This approach divides the KV cache into
125 fixed-size pages, allowing for more efficient memory allocation and management. By doing so,
126 PagedAttention enables better utilization of GPU memory, reducing fragmentation and allowing for
127 longer context windows without sacrificing performance.
128

129 Quest (Tang et al., 2024) and ArkVale (Chen et al., 2024a) are two query-aware criticality estimation
130 algorithms built on the PagedAttention. They effectively identify critical KV-cache tokens and
131 perform self-attention selectively on the chosen tokens. For each page, Quest and ArkVale calculate
132 an upper bound using the feature values of the Key vector for each page’s criticality estimation. Given
133 all criticality scores of the pages, Top-K pages are chosen to perform approximate self-attention,
134 where K is a preset constant (e.g. 128, 256). Additionally, ArkVale integrates the GPU-CPU
135 offloading into the system to further save GPU memory. However, the main issue with both Quest and
136 ArkVale is that they make all tokens in the query head attend to the same key/value blocks activated
137 by sparse attention, which is too coarse-grained, as the information each token needs to attend to can
138 vary significantly. Instead, IceCache allows each query head to attend to different key/value blocks,
139 which makes the attention-approximation more accurate.
140

141

3 BACKGROUND

142

143

3.1 ATTENTION MECHANISM AND SPARSE ATTENTION

144

145 Mathematically, the attention operation takes three matrices as input, $\mathbf{K} \in \mathbb{R}^{m \times d}$, $\mathbf{Q} \in \mathbb{R}^{n \times d}$, $\mathbf{V} \in$
146 $\mathbb{R}^{m \times d'}$, which denote keys, queries and values, respectively. Optionally, it may also take in a mask
147 as input, $\mathbf{S} \in \mathbb{R}^{n \times m}$, whose entries are either 0 or 1. The i th rows of \mathbf{K} , \mathbf{Q} and \mathbf{V} , denoted as \mathbf{k}_i ,
148 \mathbf{q}_i and \mathbf{v}_i , represent the i th key, query, and value respectively. The entry of \mathbf{S} in the i th row and j th
149 column, denoted as $s_{i,j}$, represents whether the i th query is allowed to attend to the j th key — if it is
150 1, it would be allowed; if it is 0, it would not be. A common masking scheme is the causal mask,
151 where $s_{i,j}$ is 1 if $i \geq j$ and 0 otherwise. Keys and queries have the same dimension d , and each key
152 is associated with a value, and so the number of keys and values is the same and denoted as m . The
153 attention operation computes the attention weight matrix $\mathbf{A} \in \mathbb{R}^{n \times m}$. Its entry in the i th row and j th
154 column, denoted as $a_{i,j}$, is computed with the following formula:
155

$$a_{i,j} = \frac{s_{i,j} \exp\left(\frac{\mathbf{q}_i^\top \mathbf{k}_j}{\sqrt{d}}\right)}{\sum_{j'=1}^m s_{i,j'} \exp\left(\frac{\mathbf{q}_i^\top \mathbf{k}_{j'}}{\sqrt{d}}\right)} \quad (1)$$

156 The attention matrix \mathbf{A} is typically sparse (Nikita et al., 2020; Gupta et al., 2021), i.e., in each row of
157 \mathbf{A} , only a few attention weights have significant (large) values, while the majority of the remaining
158 values are close to zero. If we can somehow identify the k unmasked keys that receive the highest
159 attention weights for each query \mathbf{q}_i without computing the attention weights for all keys, the original
160 attention matrix \mathbf{A} can be approximated by only computing the inner product for the identified keys,
161 which can save a significant amount of computational resources.
162

162 3.2 GENERATIVE INFERENCE OF LLM
163164 The generative inference process of LLMs primarily comprises two key stages: the prefill (or prompt)
165 stage and the decoding (or generation) stage.166 In the prefill stage, the model takes an input prompt sequence of length s_{in} and processes it through
167 all layers of the LLM. During this process, the keys and values for each token in the sequence are
168 computed and stored as part of the KV cache. The decoding stage begins once the prompt has been
169 processed. Here, the model generates output tokens one step at a time, using and updating the KV
170 cache iteratively. For each decoding step, the current token’s computation depends on the stored keys
171 and values from previous tokens, allowing the model to maintain context over the sequence. The KV
172 cache thus plays a crucial role in enabling efficient autoregressive generation by reducing redundant
173 computations and maintaining information about past tokens.174 3.3 MULTI-LEVEL DCI
175176 **Prioritized Dynamic Continuous Indexing (P-DCI)** Li & Malik (2017) propose an exact, random-
177 ized algorithm designed to perform efficient k -nearest neighbour (k-NN) searches in high-dimensional
178 spaces. Unlike traditional methods that rely on space partitioning, P-DCI avoids this by constructing
179 multiple indices, each imposing an ordering of all data points based on their projections onto random
180 vectors. During querying, P-DCI maintains a priority queue to process points in an order that is
181 likely to find nearer neighbours sooner. It computes a dynamic lower bound on the distance to the
182 nearest neighbour, allowing early termination of the search when the bound exceeds the distance to
183 the current best candidates. This approach significantly reduces the number of distance evaluations
184 and memory usage compared to methods like Locality-Sensitive Hashing (LSH).185 **Multi-level Dynamic Continuous Indexing (M-DCI)** Mao et al. (2024) extend P-DCI by introducing
186 a hierarchical structure to further enhance search efficiency. The index is organized into multiple
187 levels, where each level contains a subset of data points. Points are randomly promoted to higher
188 levels, forming a pyramid-like structure. Each point at a lower level is assigned a parent in the next
189 higher level, typically the nearest neighbour among the promoted points. This creates “nodes” or
190 clusters of points sharing the same parent. When querying, the algorithm starts at the top level,
191 using P-DCI to find the k -closest points to the query. It then recursively searches within the nodes
192 associated with these points at the next lower level, continuing this process down the hierarchy. This
193 multi-level approach allows M-DCI to focus computational resources on the most promising regions
194 of the index, effectively narrowing down the search space and improving query times, especially in
195 indexes with high intrinsic dimensionality.

196 4 ICECACHE

197 We propose an innovative approach, named IceCache, that integrates token clustering with KV-
198 cache storage. Our method consists of three steps: (1) Indexing; (2) Page Selection; and (3) Bulk
199 Back-loading. The Indexing step occurs either during the prompt processing phase—when IceCache
200 constructs a hierarchical tree structure, referred to as the DCI-tree, for the prompt key embeddings; or
201 when new window pages are offloaded to the CPU. In this step, similar tokens are grouped into units
202 called nodes, rather than being stored sequentially in virtual memory pages as in PagedAttention.
203 Here, a node denotes a group of data points that share the same parent in the tree hierarchy. The
204 next two steps take place during the token generation (decoding) phase. In the Page Selection
205 step, IceCache employs a fast Approximate Nearest Neighbor (ANN) search algorithm, P-DCI, to
206 independently select the top- k most relevant key pages for each attention head. Finally, in the Bulk
207 Back-loading step, the selected pages are efficiently transferred from the CPU back to the GPU.
208 IceCache overlaps the DCI Indexing (a CPU-intensive operation) with ongoing GPU computations,
209 thereby minimizing additional latency.210 We provide further details on each of these three steps in the following subsections and illustrate the
211 method in Fig 2.212 4.1 INDEXING: CLUSTERING KEY EMBEDDINGS INTO A HIERARCHICAL TREE
213214 PagedAttention (Kwon et al., 2023) is a memory management strategy designed to optimize attention
215 computation in LLMs by organizing key-value pairs into sequential memory pages. It stores these
key-value pairs based on their original token indices, ensuring that tokens appearing consecutively

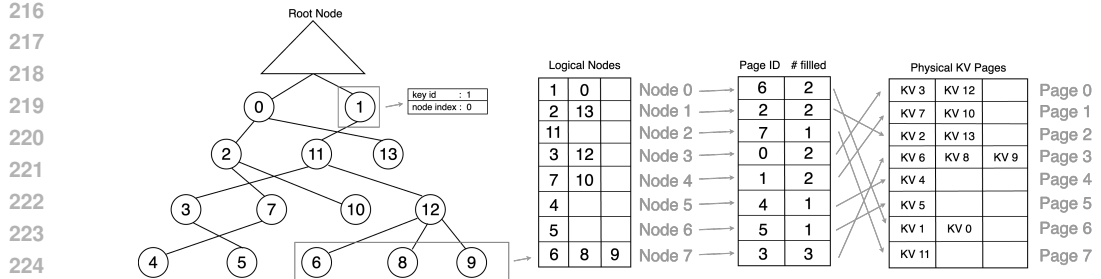


Figure 2: Illustration of DCI-tree and IceCache: The hierarchical structure on the left visualizes the result of indexing key embeddings, DCI-tree, where each tree node stores metadata for the tokens such as the key ID and node index. The tables on the right depict the mapping between nodes in the DCI-tree and the corresponding pages in physical memory. For each selected node, a mapping table is used to locate the memory region containing the associated key-value embeddings.

in the input sequence are placed contiguously in memory. This organization minimizes memory fragmentation, allowing for more efficient memory access during decoding and ultimately improving computational throughput. To inherit the benefits of PagedAttention, several subsequent KV-cache optimization techniques, such as Quest (Tang et al., 2024) and ArkVale (Chen et al., 2024a), have been developed based on its principles. These methods focus on estimating the importance of each page during KV-cache selection to approximate attention computation more efficiently.

IceCache also organizes key-value embeddings into pages, but takes a fundamentally different approach during its Indexing stage. Instead of relying on the token’s original order, IceCache constructs a separate hierarchical tree structure for each attention head, called a DCI-tree, which clusters tokens based on the semantic similarity of their key embeddings. Each node in the DCI-tree represents a small group of semantically related tokens that share a common parent, effectively forming a localized cluster. From a memory system perspective, IceCache maps each node directly to a memory page, thereby preserving semantic locality in storage and enabling efficient access during decoding.

By clustering semantically similar tokens into the same nodes/pages, IceCache enables more targeted and efficient retrieval during decoding. In contrast, methods like Quest, Arkvale, or PQCache (Zhang et al., 2024a) construct pages based on the original token order, which often causes tokens relevant to a given query to be scattered across multiple pages. Retrieving them requires loading entire pages filled with many irrelevant tokens, resulting in unnecessary memory overhead. IceCache mitigates this inefficiency by grouping similar tokens, so relevant tokens tend to be concentrated within fewer pages. As a result, it achieves comparable or improved performance while reducing the number of pages retrieved.

Moreover, the DCI-tree structure used by IceCache is designed for efficient incremental updates. As new windows of tokens (e.g., from a sliding window in long-context scenarios) are offloaded to the CPU, each token is inserted into the appropriate node in the DCI-tree based on its key embedding. When a node exceeds the maximum page size, new pages are dynamically allocated to maintain balance. This adaptive tree maintenance ensures that the index remains both semantically meaningful and efficient, making IceCache particularly effective for long-sequence generation.

In summary, while prior methods treat KV-cache page layout as a static memory allocation problem, IceCache introduces a dynamic, semantically-aware structure that preserves key similarity across time. This enables more focused page retrieval, reduces memory fragmentation, and supports more efficient decoding. Furthermore, by performing indexing during the prompt or CPU offloading phase, IceCache amortizes the tree construction cost and avoids incurring additional latency during inference.

4.2 PAGE SELECTION: HEAD-SPECIFIC ANN SEARCH WITH FINE-GRAINED RETRIEVAL

During the decoding phase, given a query, IceCache performs a head-specific page selection to identify the most relevant key pages for each attention head. Leveraging the hierarchical DCI-tree

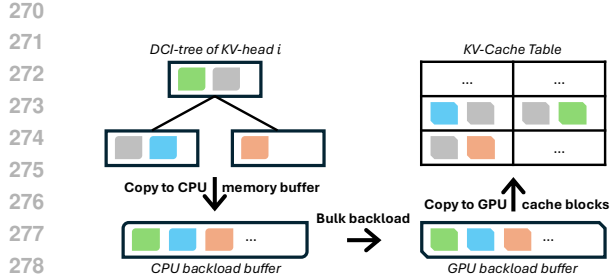


Figure 3: After IceCache selects important KV-pages, it aggregates all selected pages into a contiguous CPU preloading buffer. This buffer is then transferred via high-throughput PCIe transaction to a pre-allocated GPU buffer. Finally, the transferred blocks are scattered into their exact locations in the KV-Cache table. This bulk transfer avoids many small PCIe copies and significantly improves utilization.

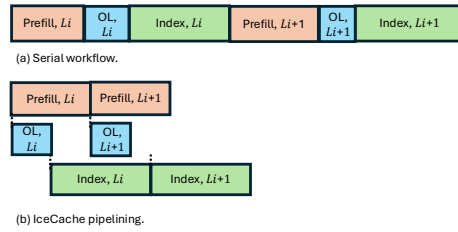


Figure 4: (a) Baseline serial workflow, where prefetching, offloading (OL), and indexing are executed strictly in sequence. (b) IceCache pipelining, where GPU prefetching overlaps with KV-offloading via PCIe and CPU-side DCI indexing. Once KVs of layer i (Li) arrive in CPU memory, Li -DCI indexing progresses in parallel with GPU prefetching and offloading of the subsequent layer ($Li+1$). This results in significantly reduced end-to-end prefetching latency.

built during indexing, we apply a fast ANN search method mentioned in Section 3.3, M-DCI, to find the top- k pages that are closest to the current query embedding for each head independently.

This design contrasts sharply with prior methods like Quest and PQCache, which either retrieve all pages indiscriminately or use a coarse global selection strategy shared across heads. In contrast, IceCache’s head-specific search recognizes that different heads often attend to different semantic aspects of the input, and thus benefit from customized retrieval strategies. This per-head granularity leads to improved attention relevance and overall model accuracy.

4.3 BULK LOADING AND PIPELINING

In this section, we present how we optimize the efficiency of the IceCache workflow, using bulk loading and pipelining. Our key observation is that the selected KV cache pages are not continuous in either main memory or GPU memory. As a result, individual transfer of these pages between main memory and GPU memory is highly inefficient. To overcome this issue, we designed bulk loading algorithms to efficiently offload and backload the selected pages, using two CPU and GPU backlog buffers. In addition, we carefully designed an efficient pipeline of prefetching calculations, KV cache offloading, and DCI indexing, for efficient prefetching.

We illustrate our bulk back-loading workflow in Figure 3. Offloading follows the same but reversed procedure. After identifying the most relevant pages (indicated by color), we filter out those already resident in GPU memory from previous token generations. The remaining pages are then aggregated into a pre-allocated CPU-memory buffer, enabling a single high-throughput PCIe transfer into a pre-allocated GPU-memory buffer. Once the pages arrive in GPU memory, we scatter them directly into their corresponding entries in the KV-Cache table.

Figure 4(b) illustrates the IceCache prefetching pipelining (other minor stages are omitted for simplicity). After the KV states are generated on the GPU, we simultaneously trigger the prefetching calculation and the offloading transfer. The DCI index construction starts building the index along with the prefetching calculation, right after the KV states fully arrive in the main memory. This approach allows the offloading and indexing latencies to be largely hidden by the main prefetching computation. Furthermore, IceCache can be easily extended with critical page reuse techniques (Liu et al., 2023; Hao et al., 2025) to further accelerate prefetching.

324 5 EXPERIMENTS

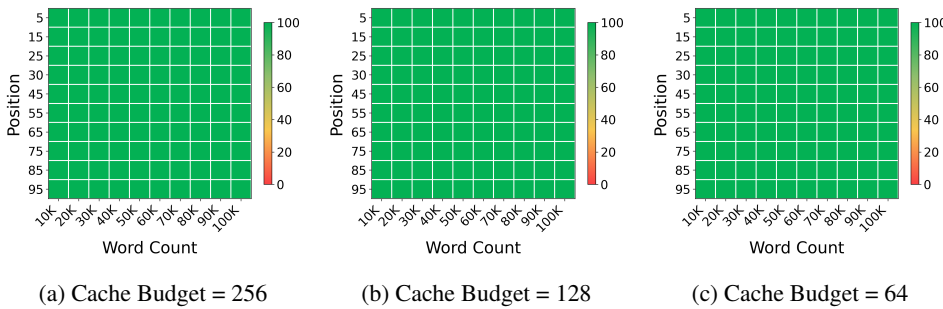
326 5.1 SETTINGS

328 We apply our method to Llama-3.1-8B-Instruct and Mistral-7B-Instruct-v0.2, two of the most popular
 329 open-source LLMs employing group-query attention (GQA) (Ainslie et al., 2023). We also test
 330 our method on a larger model, Qwen3-32B, and a multi-head attention model (Vaswani et al.,
 331 2017), LongChat-7B-v1.5. We first evaluate the recall in retrieving important tokens, followed by
 332 performance testing on 16 tasks from Longbench benchmark (Bai et al., 2023). As prior research
 333 indicates, the initial layers of the model exhibit relatively low sparsity. Therefore, neither IceCache
 334 nor baseline methods are applied to the first two layers of the models.

335 Our experimental platform comprises an Intel(R) Xeon(R) Gold 6348 CPU @ 2.60GHz and an
 336 NVIDIA A100 40GB PCIe GPU (for small models) or an NVIDIA H100 80GB PCIe GPU (for large
 337 models). The software stack includes CUDA version 12.1, PyTorch version 2.5.1, and HuggingFace
 338 Transformers version 4.51.0. We implement IceCache on top of HuggingFace Transformers, utilizing
 339 FlashInfer for the attention kernel operation.

340 5.2 PASSKEY RETRIEVAL ACCURACY

342 We first evaluate IceCache’s effectiveness in handling long-range dependencies using the passkey
 343 retrieval task (Mohtashami & Jaggi, 2023). We consider context lengths from 10k words to 100k
 344 words, and test with the size of cache budget = {256, 128, 64}. For each length, 100 test cases are
 345 generated with passkeys inserted at various positions from 0% to 95% of the total context length in
 346 increments of 5%. The results are illustrated in Fig. 5. As shown in the figure, IceCache dynamically
 347 assess the importance of evicted pages and recall crucial ones on demand, consistently maintaining
 348 100% retrieval accuracy across all tested budget sizes.



360 Figure 5: Passkey retrieval accuracy of IceCache on Llama3.1-8B-Instruct. The horizontal axis
 361 indicates the relative insertion position (%) of the passkey, while the vertical axis represents the
 362 context length in words. Results are presented for cache budgets of 256, 128, and 64. Notably,
 363 IceCache achieves 100% retrieval accuracy across all tested budget sizes.

364 5.3 LONGBENCH EVALUATION

366 To assess the performance of our method in long-context scenarios, we conduct a comprehensive
 367 evaluation on the LongBench benchmark. We compare IceCache (ICE) against six state-of-the-art KV
 368 cache optimization methods, including MagicPig (MPG) (Chen et al., 2024b), ArkVale (AKV) Chen
 369 et al. (2024a), SnapKV (SKV) Li et al. (2024b), StreamingLLM (SLM) Tang et al. (2024), OmniKV
 370 (OKV) Hao et al. (2025) and PQCache (PQC) Zhang et al. (2024a) as baselines. We also include
 371 the results of full KV cache (FULL) and ground-truth top- k KV cache (TOP- k) as baselines. The
 372 detailed results are presented in Table 1.

374 **Performance on Llama-3.1-8B-Instruct.** On Llama-3.1-8B, the effectiveness of IceCache is
 375 particularly pronounced. Most impressively, with a highly constrained KV Cache budget of just
 376 64, our method achieves an average accuracy of 47.8. This result alone surpasses the strongest
 377 baseline, PQCache, which scores 47.3 while operating with a 4 times larger budget of 256. This
 highlights the exceptional efficiency of our approach in low-resource environments. As we increase

378 Table 1: Accuracy comparison of our method (ICE) with SnapKV (SKV), SteamingLLM (SLM),
 379 OmniKV (OKV), MagicPig (MPG), PQCache (PQC), ArkVale (AKV), Full KV (FULL) and ground-
 380 truth top- k (TOP- k) on LongBench for Llama-3.1-8B-Instruct and Mistral-7B-Instruct. IceCache
 381 generally outperforms other methods across various KV cache budgets and LLMs.

Budget	Method	Single-Document QA			Multi-Document QA			Summarization			Few-shot Learning			Synthetic		Code		Avg.	
		NrtvQA 18409	Qasper 3619	MF-en 4559	HotpotQA 9151	2WikiMQA 4887	Musique 11214	GovReport 8734	QMSum 10614	MultiNews 2113	TREC 5177	TriviaQA 8209	SAMSum 6258	PCount 11141	PRe 9289	Lcc 1235	RB-P 4206		
Llama-3.1-8B-Instruct																			
N/A	FULL	30.2	45.5	54.9	55.5	46.7	31.3	35.2	25.2	27.2	72.5	91.7	43.8	8.4	99.5	65.1	58.8	49.5	
256	TOP- k	30.7	44.7	55.4	55.0	46.5	31.7	34.8	25.1	26.8	71.5	92.2	44.8	7.8	100.0	67.1	63.6	49.8	
	SKV	23.7	27.3	46.3	52.3	40.8	24.2	19.2	22.6	19.2	29.0	84.1	39.0	8.6	97.5	57.3	56.2	40.8	
	SLM	17.0	23.2	25.7	21.0	29.3	6.8	20.8	17.5	20.7	45.5	84.3	41.2	5.0	71.5	59.5	47.5	33.5	
	OKV	27.2	40.7	52.8	55.1	45.6	29.7	27.6	23.0	25.4	72.5	88.9	40.4	5.6	94.5	60.8	51.5	46.3	
	MPG	25.5	39.9	51.8	51.4	39.5	25.7	33.9	23.5	25.9	65.5	84.0	37.0	7.8	99.5	47.4	44.8	44.6	
256	PQC	28.7	43.3	52.2	55.2	45.1	28.4	27.2	24.0	22.8	69.5	91.1	41.2	6.2	99.0	59.0	54.4	47.3	
	AKV	26.1	35.2	47.5	51.6	45.6	28.1	22.9	22.5	53.5	90.1	40.0	6.7	85.0	57.7	48.9	42.8		
	64	ICE	27.4	43.2	55.7	55.3	44.4	31.2	33.4	23.7	26.2	72.5	90.3	41.9	6.6	99.5	61.7	51.6	47.8
	128	ICE	30.0	44.7	56.5	55.0	45.4	30.0	33.5	24.3	26.5	73.0	91.3	42.4	6.5	100.0	61.5	56.7	48.6
	256	ICE	30.6	44.7	56.3	55.2	45.9	30.6	34.6	24.4	26.7	73.0	92.0	43.5	6.7	100.0	62.5	56.4	49.0
Mistral-7B-Instruct-v0.2																			
N/A	FULL	26.8	33.1	49.3	42.8	27.3	18.8	33.0	24.2	27.1	71.0	86.2	42.8	2.9	87.0	56.9	54.3	42.2	
256	TOP- k	26.2	31.3	48.9	40.0	26.2	19.6	33.3	24.2	27.1	73.0	86.6	43.3	2.3	82.9	59.0	57.3	42.6	
	SKV	18.3	15.1	38.3	30.4	19.2	13.8	16.5	21.4	19.9	32.0	81.7	38.1	4.0	59.1	49.0	51.8	31.8	
	SLM	14.2	12.3	26.4	23.2	14.8	10.1	17.5	19.8	19.8	51.0	80.5	39.9	4.0	15.6	52.0	45.4	27.8	
	OKV	16.5	22.8	43.8	34.7	19.2	16.6	24.4	22.0	24.8	70.5	81.7	38.6	3.1	35.2	36.5	38.4	33.0	
	MPG	21.0	28.0	46.5	38.4	19.5	17.5	30.8	23.3	25.8	70.0	83.7	39.5	2.5	85.0	49.4	48.3	39.1	
256	PQC	21.0	25.8	42.5	18.1	20.3	16.0	29.5	21.7	27.1	70.0	85.8	39.7	2.5	75.5	54.2	49.2	37.4	
	AKV	18.0	15.2	41.5	30.7	17.0	13.2	21.6	21.6	23.1	58.0	85.8	40.6	2.1	41.5	51.4	47.2	33.0	
	64	ICE	23.9	29.0	47.4	40.5	23.5	18.3	30.6	21.8	26.0	70.5	85.9	41.5	3.5	56.5	53.2	50.4	39.0
	128	ICE	25.1	30.5	48.7	40.4	26.7	18.7	30.3	22.0	26.1	70.5	85.7	42.4	3.4	70.2	53.6	51.5	40.4
	256	ICE	25.2	31.0	48.4	40.4	26.0	18.3	31.5	23.1	26.9	71.0	86.3	42.8	3.9	85.1	54.7	53.2	41.7

400 Table 2: Accuracy comparison of our method (ICE) with Full KV (FULL) on LongBench for Qwen3-
 401 32B and LongChat-7B-v1.5.

Budget	Method	Single-Document QA			Multi-Document QA			Summarization			Few-shot Learning			Synthetic		Code		Avg.	
		NrtvQA 18409	Qasper 3619	MF-en 4559	HotpotQA 9151	2WikiMQA 4887	Musique 11214	GovReport 8734	QMSum 10614	MultiNews 2113	TREC 5177	TriviaQA 8209	SAMSum 6258	PCount 11141	PRe 9289	Lcc 1235	RB-P 4206		
Qwen3-32B																			
N/A	FULL	32.6	45.5	50.4	59.6	56.0	40.1	33.2	23.9	25.2	72.0	70.8	37.1	18.0	100.0	12.4	18.4	43.4	
256	TOP- k	28.8	43.9	50.9	61.4	55.8	38.8	30.8	23.8	24.3	71.0	70.0	35.7	15.0	97.0	10.5	17.3	42.2	
	64	ICE	29.5	43.9	50.9	61.4	55.8	38.8	30.8	23.8	24.3	71.0	70.0	35.7	15.0	97.0	10.5	17.3	42.2
	128	ICE	32.1	44.8	53.3	61.6	54.6	38.5	31.0	23.6	24.8	72.0	70.3	36.2	15.5	100.0	10.7	17.3	42.6
256	256	ICE	32.2	44.1	51.9	60.2	55.1	38.9	32.4	24.3	24.7	71.5	70.7	37.4	16.5	100.0	11.8	18.0	43.1
LongChat-7B-v1.5																			
N/A	FULL	20.8	29.4	43.1	33.0	24.4	14.7	30.8	22.8	26.7	66.5	84.0	22.5	0.0	30.5	54.7	59.2	35.2	
256	TOP- k	18.5	26.9	40.6	34.2	22.7	14.0	29.3	20.9	25.6	66.5	84.3	21.9	1.5	26.1	52.5	56.8	33.9	
	64	ICE	19.9	27.7	40.9	33.9	24.2	14.4	28.6	21.8	25.9	66.5	84.2	22.3	1.5	27.3	52.6	57.7	34.3
	128	ICE	20.4	29.5	43.0	34.6	23.7	14.2	29.8	22.7	26.1	66.5	84.7	22.9	0.0	28.5	53.6	59.0	35.0

404 the budget for IceCache to 256, its performance climbs to an average score of 49.0. This not only
 405 represents a substantial 1.7 point improvement over PQCache but also closes the performance gap to
 406 the unconstrained Full KV-Cache (49.5) to a mere 0.5 points. Notably, our performance is remarkably
 407 close to the ground-truth Top- k , demonstrating a near-optimal cache management strategy across a
 408 diverse set of tasks.

414 **Performance on Mistral-7B-Instruct.** This strong performance trend is consistent on the Mistral-
 415 7B model, confirming the robustness of our method. With a budget of 256, IceCache achieves an
 416 average accuracy of 41.7, establishing a significant 2.6 point lead over the best-performing baseline,
 417 MagicPig (39.1). Again, the low-budget capability of IceCache stands out; with a budget of 64,
 418 IceCache scores 39.0, remaining highly competitive with the top baseline (MagicPig, scores 39.1)
 419 that uses four times the cache size (256).

420 **Performance on two additional LLMs.** We evaluate IceCache on LongBench using two additional
 421 models: Qwen3-32B, a large-scale model, and LongChat-7B-v1.5, which employs standard multi-
 422 head attention rather than group-query attention. As shown in Tables 2, for Qwen3-32B, IceCache
 423 with a small budget of 64 achieves an average accuracy of 42.2 on LongBench, retaining 97.2% of the
 424 full KV cache performance (43.4). This score rises to 99.3% with a budget of 256, nearly matching
 425 the vanilla model. Similarly, on LongChat-7B-v1.5, our method preserves 96.3% of the full KV cache
 426

432 performance with a budget of 64, and achieves up to 99.4% at a budget of 256. These results provide
 433 strong evidence that IceCache is effective across different model scales and attention mechanisms.
 434

435 5.4 GSM8K COT REASONING

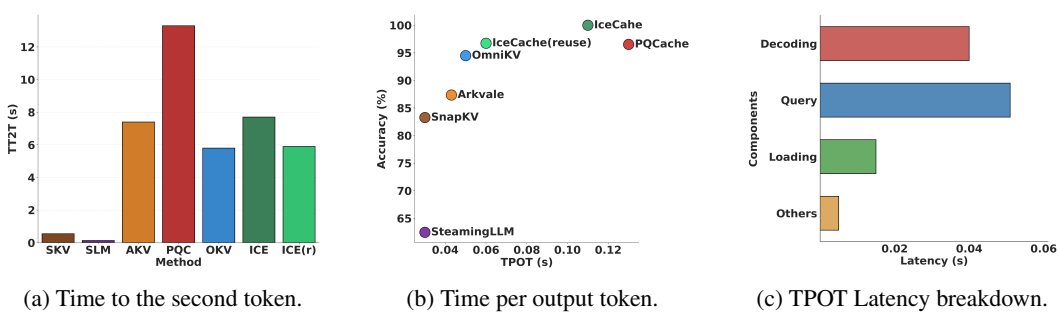
437 We also evaluate IceCache on the GSM8K benchmark using Chain-
 438 of-Thought prompting, applying a 10% budget for all compared
 439 methods using Mistral-7B-Instruct-v0.2. As shown in Table 3, Ice-
 440 Cache demonstrates superior performance, achieving an accuracy of
 441 47.4%, significantly higher than all other methods under the same
 442 budget constraint. In particular, it improves the accuracy of 46% of
 443 the strongest baseline, PQCache, by 2.6% of the original value to
 444 47.4%. Moreover, our approach nearly matches the full KV-cache
 445 (48.2%), highlighting the effectiveness of IceCache.
 446

447 5.5 LATENCY ANALYSIS

448 Since most baselines, including IceCache, use the entire KV cache to generate the first token, we
 449 follow PQCache (Zhang et al., 2024a) and report the Time to the second token (TT2T) in Fig. 6a, for a
 450 36k sequence length and all the methods compared in Table 1 except MagicPig, which is restricted to
 451 costly AVX-512 CPUs. All reported numbers in this section are obtained using Llama-3.1-8B-Instruct.
 452 Our method, IceCache, achieves competitive latency among retrieval-based algorithms, recording 7.7
 453 seconds. Its variant, IceCache (reuse), which reuses the KV-cache across layers, further reduces this
 454 to 5.9 seconds, matching OmniKV (5.8 s) and outperforming other retrieval-based baselines such as
 455 Arkvale (7.4 s) and PQCache (13.3 s). Although eviction-based methods like SnapKV (0.55 s) and
 456 StreamingLLM (0.13 s) are much faster, their speed often comes at the cost of accuracy. Overall,
 457 IceCache and IceCache(reuse) offer a strong balance between efficiency and accuracy, with the reuse
 458 variant showing how our approach can further optimize latency without significantly sacrificing
 459 performance. We include more details of IceCache(reuse) in the appendix C.

460 Similarly, for decoding latency, Fig. 6b shows the average time per generated token, along with the
 461 corresponding accuracy percentage relative to the full KV-cache model, for an input sequence length
 462 of 36k. Eviction-based methods, StreamingLLM and SnapKV (both are 0.03 seconds per token),
 463 continue to show the fastest speeds due to their minimal overhead. Among the more accurate retrieval-
 464 based methods, IceCache(reuse) achieves a highly competitive decoding time of 0.06 seconds per
 465 token – substantially faster than PQCache (0.13 s) and nearly matching the speed of OmniKV (0.05
 466 s). Vanilla IceCache maintains a strong balance, combining superior accuracy with efficient decoding.
 467 It achieves the highest accuracy percentage (99.0%) while still outperforming PQCache in speed.
 468 These results further demonstrate that IceCache effectively balances accuracy and decoding latency.
 469

470 Figure 6c presents a detailed breakdown of TPOT latency for IceCache at a sequence length of 36k,
 471 with a total latency of 0.11 seconds. In this figure, “Loading”, “Query”, and “Decoding” correspond to
 472 the overhead from CPU–GPU communication, DCI-query operations, and the overall LLM decoding
 473 process, respectively. The largest contributors to latency are the DCI-query module (0.05 s) and
 474 decoding (0.04 s), while GPU–CPU offloading and other miscellaneous operations add only 0.015
 475 seconds and 0.005 seconds, respectively.



484 Figure 6: Latency comparison of IceCache and baseline methods on a 36k-token sequence.
 485

Table 3: GSM8K CoT.

Method	Budget	Accuracy
FULL	N/A	48.2
SKV	10%	44.7
SLM	10%	44.4
OKV	10%	42.7
MPG	10%	43.1
PQC	10%	46.2
AKV	10%	30.9
ICE	10%	47.4

486 **6 CONCLUSION**

487 This paper addresses the critical challenge of managing long contexts in LLMs, where the expanding
 488 KV-cache severely impacts memory efficiency and computational performance. To address this, we
 489 introduce a novel hierarchical database, the DCI-tree, enabling lightweight updates and dynamic token
 490 management for efficient KV-cache handling. Building on this, we propose IceCache, an end-to-end
 491 page-based KV-cache manager with efficient GPU–CPU offloading and recall. Extensive experiments
 492 across diverse long-context tasks demonstrate IceCache’s efficacy: it achieves over 99% accuracy with
 493 a 256-token budget and about 97% accuracy even with only a 64-token budget, surpassing existing
 494 baselines while using just 25% of the KV-cache token budget. These results establish IceCache as a
 495 scalable and practical solution for optimizing KV-cache in LLMs with long context requirements,
 496 delivering state-of-the-art accuracy and efficiency without sacrificing performance.

497 **REFERENCES**

500 Joshua Ainslie, James Lee-Thorp, Michiel De Jong, Yury Zemlyanskiy, Federico Lebrón, and Sumit
 501 Sanghi. Gqa: Training generalized multi-query transformer models from multi-head checkpoints.
 502 *arXiv preprint arXiv:2305.13245*, 2023.

503 Yushi Bai, Xin Lv, Jiajie Zhang, Hongchang Lyu, Jiankai Tang, Zhidian Huang, Zhengxiao Du, Xiao
 504 Liu, Aohan Zeng, Lei Hou, et al. Longbench: A bilingual, multitask benchmark for long context
 505 understanding. *arXiv preprint arXiv:2308.14508*, 2023.

506 Renze Chen, Zhuofeng Wang, Beiquan Cao, Tong Wu, Size Zheng, XiuHong Li, Xuechao Wei,
 507 Shengen Yan, Meng Li, and Yun Liang. Arkvale: Efficient generative llm inference with recallable
 508 key-value eviction. In *The Thirty-eighth Annual Conference on Neural Information Processing
 509 Systems*, 2024a.

510 Zhuoming Chen, Ranajoy Sadhukhan, Zihao Ye, Yang Zhou, Jianyu Zhang, Niklas Nolte, Yuandong
 511 Tian, Matthijs Douze, Leon Bottou, Zhihao Jia, et al. Magicpig: Lsh sampling for efficient llm
 512 generation. *arXiv preprint arXiv:2410.16179*, 2024b.

513 Ankit Gupta, Guy Dar, Shaya Goodman, David Ciprut, and Jonathan Berant. Memory-efficient
 514 transformers via top- k attention. *arXiv preprint arXiv:2106.06899*, 2021.

515 Jitai Hao, Yuke Zhu, Tian Wang, Jun Yu, Xin Xin, Bo Zheng, Zhaochun Ren, and Sheng Guo.
 516 Omnikv: Dynamic context selection for efficient long-context llms. In *The Thirteenth International
 517 Conference on Learning Representations*, 2025.

518 Woosuk Kwon, Zhuohan Li, Siyuan Zhuang, Ying Sheng, Lianmin Zheng, Cody Hao Yu, Joseph
 519 Gonzalez, Hao Zhang, and Ion Stoica. Efficient memory management for large language model
 520 serving with pagedattention. In *Proceedings of the 29th Symposium on Operating Systems
 521 Principles*, pp. 611–626, 2023.

522 Wonbeom Lee, Jungi Lee, Junghwan Seo, and Jaewoong Sim. {InfiniGen}: Efficient generative
 523 inference of large language models with dynamic {KV} cache management. In *18th USENIX
 524 Symposium on Operating Systems Design and Implementation (OSDI 24)*, pp. 155–172, 2024.

525 Ke Li and Jitendra Malik. Fast k-nearest neighbour search via prioritized dci. In *International
 526 conference on machine learning*, pp. 2081–2090. PMLR, 2017.

527 Yucheng Li, Huiqiang Jiang, Qianhui Wu, Xufang Luo, Surin Ahn, Chengruidong Zhang, Amir H
 528 Abdi, Dongsheng Li, Jianfeng Gao, Yuqing Yang, et al. Scbench: A kv cache-centric analysis of
 529 long-context methods. *arXiv preprint arXiv:2412.10319*, 2024a.

530 Yuhong Li, Yingbing Huang, Bowen Yang, Bharat Venkitesh, Acyr Locatelli, Hanchen Ye, Tianle Cai,
 531 Patrick Lewis, and Deming Chen. Snapkv: Llm knows what you are looking for before generation.
 532 *arXiv preprint arXiv:2404.14469*, 2024b.

533 Zichang Liu, Jue Wang, Tri Dao, Tianyi Zhou, Binhang Yuan, Zhao Song, Anshumali Shrivastava,
 534 Ce Zhang, Yuandong Tian, Christopher Re, et al. Deja vu: Contextual sparsity for efficient llms
 535 at inference time. In *International Conference on Machine Learning*, pp. 22137–22176. PMLR,
 536 2023.

540 Yuzhen Mao, Martin Ester, and Ke Li. Iceformer: Accelerated inference with long-sequence
 541 transformers on CPUs. In *The Twelfth International Conference on Learning Representations*,
 542 2024.

543 Amirkeivan Mohtashami and Martin Jaggi. Landmark attention: Random-access infinite context
 544 length for transformers. *arXiv preprint arXiv:2305.16300*, 2023.

545 Kitaev Nikita, Kaiser Lukasz, Levskaya Anselm, et al. Reformer: The efficient transformer. In
 546 *Proceedings of International Conference on Learning Representations (ICLR)*, 2020.

547 Luka Ribar, Ivan Chelombiev, Luke Hudlass-Galley, Charlie Blake, Carlo Luschi, and Douglas Orr.
 548 Sparq attention: Bandwidth-efficient llm inference. *arXiv preprint arXiv:2312.04985*, 2023.

549 Jiaming Tang, Yilong Zhao, Kan Zhu, Guangxuan Xiao, Baris Kasikci, and Song Han. Quest:
 550 Query-aware sparsity for efficient long-context llm inference. *arXiv preprint arXiv:2406.10774*,
 551 2024.

552 Ashish Vaswani, Noam Shazeer, Niki Parmar, Jakob Uszkoreit, Llion Jones, Aidan N Gomez, Łukasz
 553 Kaiser, and Illia Polosukhin. Attention is all you need. *Advances in neural information processing
 554 systems*, 30, 2017.

555 Jason Wei, Xuezhi Wang, Dale Schuurmans, Maarten Bosma, Fei Xia, Ed Chi, Quoc V Le, Denny
 556 Zhou, et al. Chain-of-thought prompting elicits reasoning in large language models. *Advances in
 557 neural information processing systems*, 35:24824–24837, 2022.

558 Guangxuan Xiao, Yuandong Tian, Beidi Chen, Song Han, and Mike Lewis. Efficient streaming
 559 language models with attention sinks. *arXiv preprint arXiv:2309.17453*, 2023.

560 Hailin Zhang, Xiaodong Ji, Yilin Chen, Fangcheng Fu, Xupeng Miao, Xiaonan Nie, Weipeng Chen,
 561 and Bin Cui. Pqcache: Product quantization-based kvcache for long context llm inference. *arXiv
 562 preprint arXiv:2407.12820*, 2024a.

563 Zhenyu Zhang, Ying Sheng, Tianyi Zhou, Tianlong Chen, Lianmin Zheng, Ruisi Cai, Zhao Song,
 564 Yuandong Tian, Christopher Ré, Clark Barrett, et al. H2o: Heavy-hitter oracle for efficient
 565 generative inference of large language models. *Advances in Neural Information Processing
 566 Systems*, 36, 2024b.

567

568

569

570

571

572

573

574

575

576

577

578

579

580

581

582

583

584

585

586

587

588

589

590

591

592

593

594 **A METHOD OVERVIEW**
 595

596 We separate all tokens into three groups: *sink tokens*, which are the tokens at the very beginning of
 597 the input sequence; *window tokens*, which are the most recent tokens; and all the remaining tokens in
 598 between. The pages that store sink tokens are referred to as *sink pages*, and those that store window
 599 tokens are referred to as *window pages*. We always keep all the sink and window pages in GPU.

600 We provide the pseudocode below for IceCache. It operates in two main phases: (1) Prefill Phase:
 601 During the initial processing of prompt tokens, IceCache allocates paged KV memory per layer and
 602 performs self-attention computations. From the third layer onward, it copies KV embeddings to CPU
 603 and builds a dynamic index – DCI-tree. This tree enables efficient future lookup of important tokens
 604 based on query embeddings. (2) Decode Phase: During autoregressive decoding, each new token’s
 605 query embedding is used to retrieve the most relevant KV pages via DCI-based query. Selected pages
 606 are back-loaded to GPU on demand, while unimportant pages are offloaded to CPU storage. When a
 607 new window page is offloaded, the DCI-tree is incrementally updated to store tokens in this page.
 608 The detailed steps are outlined in Algorithm 1. We will explain the mechanisms behind indexing and
 609 page selection in the following sections.

610 **B METHOD DETAILS**
 611

612 **B.1 INDEXING**
 613

614 For each attention head, given a set of pre-computed key embeddings, IceCache first indexes them
 615 using a hierarchical tree structure which is obtained by a novel approach called Multi-level DCI
 616 (M-DCI). It works by constructing a dynamic index called DCI-tree and applies Prioritized DCI
 617 (P-DCI) (Li & Malik, 2017) to each level of the tree recursively (more details are in Section 3.3). The
 618 data points processed in M-DCI are transformed key embeddings and query embeddings using the
 619 following transformation formulas, which we denote as $T_K : \mathbb{R}^d \rightarrow \mathbb{R}^{d+1}$ and $T_Q : \mathbb{R}^d \rightarrow \mathbb{R}^{d+1}$:

$$T_K(\mathbf{k}_j) = [\mathbf{k}_j/c \quad \sqrt{1 - \|\mathbf{k}_j\|_2^2/c^2}]^\top \quad (2)$$

$$T_Q(\mathbf{q}_i) = [\mathbf{q}_i/\|\mathbf{q}_i\|_2 \quad 0]^\top \quad (3)$$

620 where $c \geq \max_{j'} \|\mathbf{k}_{j'}\|_2$ is at least the maximum norm across all keys. We use the Euclidean distance
 621 as the distance function.

622 At the very beginning of the indexing, all data points are initially placed at the bottom level of the
 623 DCI-tree. Subsequently, some points are randomly selected to be promoted to the next higher level
 624 based on a promotion ratio $r < 1$. The ratio r is predefined during DCI-tree initialization and remains
 625 fixed throughout the process. After the indexing, we can get the total number of levels in the DCI-tree,
 626 denoted as L . The details are presented in Algorithm 2.

627 Specifically, let n_ℓ denote the number of data points at level ℓ , with level indices starting from the
 628 bottom (i.e., the lowest level is $\ell = 1$). Ideally, the number of points satisfies the recurrence relation
 629 $n_\ell = r \cdot n_{\ell-1}$. In other words, the distribution over level indices follows a geometric distribution.
 630 The probability that a point is assigned to the highest level ($\ell = L$) is r^{L-1} , while the probability of
 631 being assigned to level ℓ (for $1 \leq \ell \leq L-1$) is $r^{\ell-1} - r^\ell$.

632 After level assignment, each data point at level ℓ is linked to a parent at level $\ell + 1$, defined as the
 633 closest point in terms of key embedding distance. This parent assignment is formulated as a 1-nearest
 634 neighbor search and is efficiently solved using M-DCI query.

635 In the decoding stage, when a new token is generated, its key embedding is inserted into the
 636 appropriate position in the DCI-tree. A level ℓ is first assigned to the new key according to the same
 637 random promotion process. Then, its parent at level $\ell + 1$ is determined, and the key is added to the
 638 physical memory page corresponding to the node into which it is inserted.

639
 640 **B.2 PAGE SELECTION**
 641

642 As aforementioned, IceCache aims to accelerate self-attention by loading only a limited number of
 643 pages into GPU memory for computation. Therefore, the objective of page selection is to maximize
 644 the *recall* (or hit rate) of significant keys for a given query. By clustering semantically similar tokens

648 into the same nodes/pages, IceCache enables more targeted and efficient retrieval during decoding. In
 649 contrast, methods like Quest (Tang et al., 2024), Arkvale (Chen et al., 2024a), or PQCache (Zhang
 650 et al., 2024a) construct pages based on the original token order, which often causes tokens relevant to
 651 a given query to be scattered across multiple pages. Retrieving them requires loading entire pages
 652 filled with many irrelevant tokens, resulting in unnecessary memory overhead. IceCache mitigates
 653 this inefficiency by grouping similar tokens, so relevant tokens tend to be concentrated within fewer
 654 pages. As a result, the hit rate of significant keys during decoding increases. The detailed procedure
 655 is shown in Algorithms 3 and 4.

656 Specifically, when computing the attention matrix, given a query vector q_i , we follow the query
 657 process described in Section 3.3 to identify the top- k keys that are most likely to yield the highest
 658 dot-product values with q_i . Once these top- k keys are identified, we load only the pages that contain
 659 them. Suppose p pages are loaded, and each page contains d entries, since not all the pages are fully
 660 filled, the number of loaded keys N is bounded as: $N \leq pd$.

661 The approximate attention scores between the query q and these N selected keys are then computed
 662 using Equation 1. The masks $s_{i,j}$ are set to 1 for the selected keys and 0 for all others. Note that,
 663 IceCache constructs a separate DCI-tree for each attention head, allowing it to retrieve different sets
 664 of significant pages per head. This head-specific, fine-grained selection mechanism distinguishes
 665 IceCache from baselines such as Quest and ArkVale, which retrieve the same set of pages for all
 666 heads, potentially limiting their retrieval accuracy.

667 C DETAILS OF ICECACHE (REUSE) ON LONGBENCH

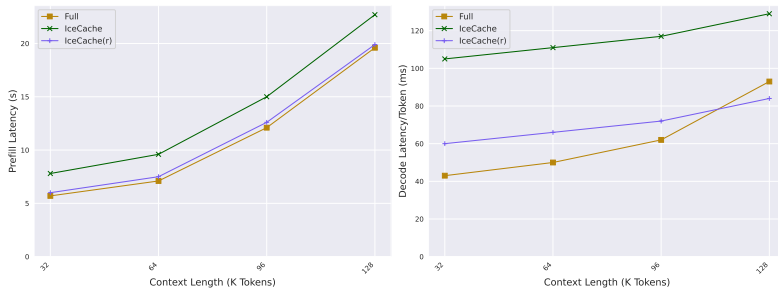
668 We present the LongBench task scores for IceCache (reuse) in Table 4. Starting from the third layer,
 669 we build the DCI-tree and perform DCI-queries every five layers; we refer to these as “anchor layers”.
 670 For the layers in between, we reuse the KV-cache indices selected at the most recent anchor layer.
 671

672 Table 4: Accuracy of IceCache (reuse) on LongBench.
 673

Budget	Method	Single-Document QA		Multi-Document QA		Summarization			Few-shot Learning		Synthetic		Code		Avg.			
		NrtvQA	Qasper	MF-en	HotpotQA	2WikiMQA	Musique	GovReport	QMSum	MultiNews	TREC	TriviaQA	SAMSum	PCount	PR	Lcc	RB-P	
Llama-3.1-SB-Instruct																		
256	ICE(r)	28.6	42.6	54.0	55.4	45.8	29.6	32.8	24.0	25.9	72.0	90.1	40.9	5.7	96.5	61.4	51.6	47.3

679 D LATENCY SCALING ACROSS CONTEXT LENGTHS

680 Figure 7 compares the prefill latency (left) and per-token decode latency (right) of Full Attention,
 681 IceCache, and IceCache(r) as the input context grows from 32K to 128K tokens. The results show
 682 that IceCache introduces only a modest overhead during prefill, while achieving better scaling than
 683 Full Attention in the decoding stage.
 684



696 Figure 7: Latency scaling across context lengths (32k, 64k, 96k and 128k). Left: IceCache and
 697 IceCache(r) maintain close prefill latency to Full-KV across all context lengths. Although IceCache
 698 performs additional CPU-side indexing, the overhead remains small relative to the overall prefill
 699 cost. Right: both IceCache variants exhibit a slower growth rate in per-token decoding latency
 700 compared to Full-KV. Full-KV’s decoding cost rises sharply with sequence length, and IceCache(r)
 701 even outperforms Full-KV at very long contexts (128k).

Algorithm 1 IceCache

```

702
703
704: Input: Sequence of tokens  $x_{1:I}$ , Transformer with  $L$  attention layers, Page size  $s$ 
705: Phase 1: Prefill
706: 3: for  $\ell = 0$  to  $L - 1$  do
707: 4:   Allocate pages and arrange KVs to the pages for layer  $\ell$ 
708: 5:   if  $\ell \geq 2$  then
709:     Copy KVs of tokens between sink tokens and window tokens from GPU to CPU (denoted
710:       as  $S_k$  and  $S_v$ )
711:   end if
712:   Compute the output from the current self-attention layer  $\ell$ 
713:   if  $\ell \geq 2$  then
714:      $T_l \leftarrow \text{DCI-INDEXING}(S_k, S_v)$ 
715:   end if
716: end for
717: Phase 2: Decode (repeated over time steps  $i > I$ )
718: 13: while receive new token  $x_i$  with  $\mathbf{q}_i$  as its query embedding do
719: 14:   for  $\ell = 0$  to  $L - 1$  do
720: 15:     if Number of tokens in the last page  $\geq s - 1$  then
721:       Offload the oldest window page  $P_w$  from GPU to CPU
722:       Set Flag to True
723:     end if
724:     Append KVs of  $x_i$  to the end of the newest window page
725:     if  $\ell \geq 2$  then
726:        $S_l \leftarrow \text{PAGE-SELECT}(\mathbf{q}_i, T_l, k)$ 
727:       Recall selected pages  $S_l$  from CPU to GPU
728:     end if
729:     Compute the output from the current self-attention layer  $\ell$ 
730:     if  $\ell \geq 2$  & Flag is True then
731:       // Insert the tokens in offloaded  $P_w$  to  $T_l$ 
732:       for  $i$  in  $P_w$  do
733:         // Random Promotion
734:          $l_i \leftarrow 1$  ▷ Start at bottom level
735:         while  $\text{Random}(0, 1) < r$  do
736:            $l_i \leftarrow l_i + 1$  ▷ Promote to the next higher level
737:         end while
738:          $\{p_i\} \leftarrow \text{QUERY}(\mathbf{k}_i, T_l, l_i, 1)$  ▷ Get the parent index using QUERY (Alg.4)
739:         Insert  $\mathbf{k}_i$  to  $T_l$  with  $p_i$  as its parent node index
740:       end for
741:     end if
742:   end if
743:    $i = i + 1$ 
744: end while
745
746
747
748
749
750
751
752
753
754
755

```

756

Algorithm 2 Indexing

757

Require: A list S_k of n keys $\mathbf{k}_1, \dots, \mathbf{k}_n \in \mathbb{R}^d$, Promotion ratio r

function DCI-INDEXING(S_k, r)

for $i = 1$ **to** n **do**

 // Random Promotion

$l_i \leftarrow 1$ ▷ Start at bottom level

while $\text{Random}(0, 1) < r$ **do**

$l_i \leftarrow l_i + 1$ ▷ Promote to the next higher level

end while

end for

 Remove the empty levels

 Initialize T with an empty root node

for $i = 1$ **to** n **do**

$\{p_i\} \leftarrow \text{QUERY}(\mathbf{k}_i, T, l_i, 1)$ ▷ Get the parent index using QUERY (Alg.4)

 Insert \mathbf{k}_i to T with p_i as its parent node index

end for

return T

end function

772

773

774

775

Algorithm 3 Page Selection

776

Require: Query vector $\mathbf{q}_i \in \mathbb{R}^d$, DCI-tree T , Number of critical keys k

function PAGE-SELECT(\mathbf{q}_i, T, k)

 Initialize $S_l \leftarrow \emptyset$

$S_k \leftarrow \text{QUERY}(\mathbf{q}_i, T, -1, k)$

$S_l \leftarrow \text{FIND-PAGE-INDEX}(S_k)$

return S_l

end function

782

783

784

785

Algorithm 4 k -Nearest Neighbour Querying

786

Require: Query vector $\mathbf{q}_i \in \mathbb{R}^d$, DCI-tree T with L levels, Target level l , Number of critical keys k

787

function QUERY(\mathbf{q}_i, T, l, k)

788

if $l = -1$ **then**

789

$l \leftarrow 1$

790

 Set Flag to True

791

else

792

 Set Flag to False

793

end if

794

$S \leftarrow \emptyset$

795

$P \leftarrow$ empty priority queue with size k

796

for $i = L$ **to** l **do**

797

$S' \leftarrow \emptyset$

798

if $i = L$ **then**

799

$S \leftarrow \{\text{root node}\}$

800

end if

801

for s **in** S **do**

802

$S'' \leftarrow \text{Prioritized-DCI-Query}(\mathbf{q}_i, s, k)$

803

$S' \leftarrow S' \cup S''$

804

end for

805

if Flag is True **or** $i = l$ **then**

806

for s **in** S' **do**

807

$P \leftarrow \text{Add-to-Priority-Queue}(P, s)$

808

end for

809

end if

$S \leftarrow S'$

810

end for

811

return k nodes in P that have the keys with maximum inner-product with \mathbf{q}_i

end function

810 **E LLM USAGE**
811812 This work focuses on optimizing KV-cache management for large language models (LLMs). All the
813 base models used in this paper can be viewed as LLMs, including Llama-3.1-8B-Instruct, Mistral-7B-
814 Instruct-v0.2, Qwen3-32B, and LongChat-7B-v1.5. We also leveraged an LLM to help refine the
815 manuscript's language and improve its overall readability.816
817
818
819
820
821
822
823
824
825
826
827
828
829
830
831
832
833
834
835
836
837
838
839
840
841
842
843
844
845
846
847
848
849
850
851
852
853
854
855
856
857
858
859
860
861
862
863